J. Fluid Mech. (2005), *vol.* 543, *pp.* 239–248.
doi:10.1017/S0022112005006518 Printed in the United Kingdom

On fine sediment transport by a flood surge

By DAVID PRITCHARD

BP Institute for Multiphase Flow, Department of Earth Sciences, University of Cambridge, Madingley Rise, Madingley Road, Cambridge CB3 0EZ, UK

(Received 12 July 2004 and in revised form 31 July 2005)

We develop asymptotic solutions for passive suspended sediment transport under a flood surge on a uniform slope. Our solutions provide predictions of the net scour under a surge, and simple estimates of the conditions under which it may 'bulk up' into a mud or debris flow, as well as illustrating their sensitivity to sediment entrainment rates.

1. Introduction and motivation

When water confined behind a barrier, for example in an artificial reservoir or a crater lake, is suddenly released, a large and swift flood surge propagates downstream. Depending on the terrain over which such a surge flows, it may be able to mobilize large quantities of sediment: understanding how this occurs is important both in order to predict how such a surge will reshape the slope or channel bed beneath it and to determine how it should be treated for the purposes of hazard assessment and prevention.

A surge which initially consists of clear water may mobilize sediment either by entraining it into suspension or as a highly concentrated layer of mobile particles (bedload). The latter mechanism is dominant for coarse sediment, and for a sufficiently large surge over a non-cohesive substrate the fluidized layer may even become comparable in thickness to the flow itself (Fraccarollo & Capart 2002). Finer, more cohesive sediment is mainly transported as suspended load, and it is this which we investigate here. We note that the two modes of transport are not exclusive, and for example a debris flow may have a muddy body and a fluidized granular 'snout' (Ancey 2001). The entrainment process is limited by the fact that, as volumetric concentrations reach around 10–20 %, turbulence is damped, the rheology changes, and the surge starts to 'bulk up' into a rapid muddy flow (see e.g. Huang & Garcia 1998). Such muddy flows propagate more slowly than surges of clear water but, because of their greater density and ability to transport large solid objects, they may also be extremely destructive (see e.g. Ancey 2001), and for hazard assessment it is useful to predict when and where they can occur. The flood surge model we develop here is valid only before this rheological transition occurs, but it allows us to draw some conclusions about the circumstances under which the transition is possible.

We will first (§ 2) discuss the formulation and validity of our model; we will then (§ 3) describe some typical results, including erosion patterns and some necessary conditions for a surge to bulk up. We make some concluding remarks in § 4.

2. Description of the model

We consider the equations for shallow flow on a bed of angle θ from the horizontal,

$$\frac{\partial \hat{h}}{\partial \hat{t}} + \frac{\partial(\bar{u}\hat{h})}{\partial \hat{x}} = 0, \qquad \frac{\partial \bar{u}}{\partial \hat{t}} + \bar{u}\frac{\partial \bar{u}}{\partial \hat{x}} + \hat{g}\cos\theta\frac{\partial \hat{h}}{\partial \hat{x}} = \hat{g}\sin\theta - \frac{c_D\bar{u}^2}{\hat{h}}. \tag{2.1}$$

Here $\hat{h}$ denotes fluid depth normal to the bed and $\bar{u}$ denotes vertically averaged flow velocity parallel to the bed. (Throughout, bars and carets identify physical variables, while rescaled dimensionless quantities are unadorned.) We have assumed a quadratic drag law suitable for turbulent flows, so the basal shear stress is given by $\hat{\tau} = c_D \hat{\rho} \bar{u}^2$, where $\hat{\rho}$ is the density of water and c_D is a small drag coefficient. We will assume that the effect of erosion on the bed is negligible: we consider the validity of this assumption below.

Weir (1983) showed that when a finite mass of water of cross-sectional area $\hat{A}$ is released on a uniform slope, the flow adjusts after a characteristic time $\hat{t}_{\mathrm{adj}}$ to a state in which the dominant dynamical balance is between the alongslope gravitational acceleration and the drag term,

$$c_D \bar{u}^2 = (\hat{g} \sin\theta)\hat{h}. \tag{2.2}$$

The adjustment time is given by

$$\hat{t}_{\mathrm{adj}} \sim \frac{\hat{A}^{1/4} c_D^{1/2}}{(\sin\theta)^{5/4} \hat{g}^{1/2}}. \tag{2.3}$$

We now define the non-dimensional variables

$$x = \hat{x}/\hat{X}, \quad t = \hat{t}/\hat{T}, \quad u = \bar{u}\hat{T}/\hat{X}, \quad h = \hat{h}/\hat{H}, \tag{2.4}$$

where the capitals denote characteristic scales which are to be determined. The continuity and (reduced) momentum equations can now be written as

$$\frac{\partial h}{\partial t} + \frac{\partial (uh)}{\partial x} = 0, \qquad u^2 = \left[\frac{\hat{H}\hat{T}^2}{\hat{X}^2} \frac{\hat{g}\sin\theta}{c_D}\right] h, \tag{2.5}$$

while the volume condition is given by

$$\int_0^{x_f(t)} h(x,t)\,\mathrm{d}x = \left[\frac{\hat{A}}{\hat{X}\hat{H}}\right], \tag{2.6}$$

where $\hat{x} = \hat{x}_f(\hat{t})$ is the position of the flow front.

Requiring that the collections of terms in square brackets in (2.5) and (2.6) should each be equal to 1, and substituting for $u(h)$ in the continuity equation, we obtain the kinematic-wave equation

$$\frac{\partial h}{\partial t} + \frac{3}{2} h^{1/2} \frac{\partial h}{\partial x} = 0 \tag{2.7}$$

and thus the degenerate kinematic-wave solution

$$u(x,t) = \frac{2}{3}\frac{x}{t}, \qquad h(x,t) = \frac{4}{9}\frac{x^2}{t^2} \quad \text{in} \quad 0 \leqslant x \leqslant k_f t^{2/3}, \qquad \text{where} \quad k_f = \frac{3}{2^{2/3}}, \tag{2.8}$$

and where all characteristics radiate from $(0,0)$. Hunt (1982) derived this solution and demonstrated that it agreed well with experiments carried out in a laboratory flume. Unlike the simple-wave solution for a dam-break flow on a horizontal surface, the solution does not lose validity as the body of the flow is invaded by a nose region in which a different dynamical balance holds (Hogg & Pritchard 2004): rather, the relative length of this nose region remains small as the current lengthens (Hunt 1984).

We now consider a transport equation for the depth-averaged volumetric concentration of suspended sediment $\bar{c} = \hat{C} c(x,t)$, where $\hat{C}$ is a characteristic scale as before. Assuming that the velocity of the flow is approximately uniform in the vertical, we may

write an advection–erosion–deposition equation (cf. Pritchard & Hogg 2002) which in non-dimensional form becomes

$$\frac{\partial c}{\partial t} + u\frac{\partial c}{\partial x} = \left[\frac{\hat{T}\hat{u}_e}{\hat{C}\hat{H}}\right]\frac{q_e(u)}{h} - \left[\frac{\hat{T}\hat{w}_s}{\hat{H}}\right]\frac{c}{h}. \tag{2.9}$$

Here $\hat{w}_s$ is the effective settling velocity of the particles and $\hat{q}_e = \hat{u}_e q_e(u)$ is a volumetric sediment entrainment rate. Assuming a given vertical distribution of sediment, the settling velocity $\hat{w}_s$ may be weighted to reflect the higher concentrations near the bed; for a well-mixed suspension it reduces to the settling velocity for an individual particle. The entrainment rate parameter $\hat{u}_e$ has the dimensions of velocity, and in many models it is taken to be proportional to $\hat{w}_s$.

2.1. *Non-dimensionalization and conditions for validity of the model*

Requiring that the terms in square brackets be set equal to 1 in equations (2.5), (2.6) and (2.9) now specifies the scaling quantities completely. We obtain

$$\hat{C} = \frac{\hat{u}_e}{\hat{w}_s}, \quad \hat{X} = \left[\frac{\hat{A}^3\hat{g}\sin\theta}{c_D\hat{w}_s^2}\right]^{1/5}, \quad \hat{H} = \left[\frac{\hat{A}^2\hat{w}_s^2 c_D}{\hat{g}\sin\theta}\right]^{1/5}, \quad \hat{T} = \left[\frac{\hat{A}^2 c_D}{\hat{w}_s^3\hat{g}\sin\theta}\right]^{1/5}. \tag{2.10}$$

We expect $\hat{C}$, $\hat{T}$ and $\hat{X}$ to give rough estimates for, respectively, the typical concentrations attained under the flow, the timescale over which suspended sediment concentrations change, and the distance the flow travels over this timescale: in the next section we will compare these estimates with the analytical solution.

It is meaningful to consider sediment transport under the kinematic-wave solution if $\hat{T} \gg \hat{t}_{\mathrm{adj}}$, in other words if

$$\left[\frac{\hat{A}^2 c_D}{\hat{w}_s^3\hat{g}\sin\theta}\right]^{1/5} \gg \frac{\hat{A}^{1/4}c_D^{1/2}}{(\sin\theta)^{5/4}\hat{g}^{1/2}} \Leftrightarrow \hat{w}_s \ll \frac{\hat{g}^{1/2}\hat{A}^{1/4}(\sin\theta)^{7/4}}{c_D^{1/2}}. \tag{2.11}$$

With typical values of $\sin\theta = 0.01$, $c_D \approx 0.003$ and $\hat{g} = 10\,\mathrm{m\,s^{-2}}$, this condition becomes $\hat{w}_s \ll 0.02\,\mathrm{m^{1/2}\,s^{-1}}\hat{A}^{1/4}$, which is readily satisfied for large surges and reasonably fine sediment; on steeper slopes it may be valid even for quite coarse particles.

Finally, we may calculate the net erosion or deposition under a surge. This may be obtained by sediment budgeting: given the volumetric packing density of particles in the bed, $\hat{\phi}$, we obtain the net deposit depth at a point as $\hat{\eta}(\hat{x}) \equiv \hat{D}\eta(x)$, where

$$\hat{D} = \frac{\hat{u}_e\hat{T}}{\hat{\phi}}, \qquad \eta(x) = \int_{(x/k_f)^{3/2}}^{\infty} [c(x,t) - q_e(u(x,t))]\,\mathrm{d}t. \tag{2.12}$$

We may neglect the effects of erosion on the bed if $|\mathrm{d}\hat{\eta}/\mathrm{d}\hat{x}| = (\hat{D}/\hat{X})|\mathrm{d}\eta/\mathrm{d}x| \ll \tan\theta$. The condition $(\hat{D}/\hat{X}) \ll \tan\theta$ is equivalent to

$$\hat{w}_s \ll \frac{\hat{g}^{1/2}\hat{A}^{1/4}(\sin\theta)^{1/2}(\tan\theta)^{5/4}\hat{\phi}^{5/4}}{c_D^{1/2}\hat{C}^{5/4}}. \tag{2.13}$$

Since $\hat{C} < \hat{\phi}$, the condition (2.13) will be satisfied whenever $\hat{T} \gg \hat{t}_{\mathrm{adj}}$, and bed level changes may in general be neglected if $|\mathrm{d}\eta/\mathrm{d}x|$ remains of order 1.

3. Results for sediment transport

3.1. *Construction of solutions for suspended sediment*

We may develop solutions to equation (2.9) by writing the flow field (2.8) in Lagrangian form, obtaining Lagrangian fluid element positions $x_L(t)$, velocities $u_L(t)$ and depths $h_L(t)$:

$$x_L(t;k) = kt^{2/3}, \qquad u_L(t;k) = \frac{2k}{3t^{1/3}}, \qquad h_L(t;k) = \frac{4k^2}{9t^{2/3}}, \tag{3.1}$$

where $k > 0$ is a labelling parameter. The shock front $x_f(t)$ is a particular case of $x_L(t)$ (corresponding to $k = k_f$) since this shock must follow the frontmost fluid element.

In Lagrangian form, the concentration equation (2.9) becomes

$$\frac{\mathrm{d}c_L}{\mathrm{d}t}(t;k) = \frac{9t^{2/3}}{4k^2}[q_e(u_L(t;k)) - c_L(t;k)]. \tag{3.2}$$

Imposing the initial condition $c_L(0;k) = c_0(k)$, we obtain the solution

$$c_L(t;k) = \exp\left[-\frac{27t^{5/3}}{20k^2}\right]\left\{c_0(k) + \int_0^t \exp\left[\frac{27\tau^{5/3}}{20k^2}\right]\frac{9\tau^{2/3}}{4k^2}q_e(u_L(\tau;k))\,\mathrm{d}\tau\right\}. \tag{3.3}$$

Since we are concerned with surges caused by the release of fluid from an initially quiescent source, we assume throughout that the initial amount of sediment in suspension is negligible, $c_0(k) = 0$.

At this stage we need to specify the form of the sediment entrainment rate $q_e(u)$. There is no universally accepted model for this, so we will consider two common choices to test how sensitive our predictions are to this component of the model. The entrainment rate for both cohesive and non-cohesive sediment is often modelled as some power of the excess shear stress above a critical value $\hat{\tau}_c$ (Dyer & Soulsby 1988; Teisson *et al.* 1993), so

$$\hat{q}_e = \hat{u}_e\left(\frac{|\hat{\tau}| - \hat{\tau}_c}{\hat{\tau}_0}\right)^{m/2}\Theta(|\hat{\tau}| - \hat{\tau}_c). \tag{3.4}$$

Here $\hat{\tau}_0$ is a reference shear stress, $m > 0$, and $\Theta(y)$ is the Heaviside step function. Employing a quadratic drag law and defining $\hat{\tau}_0 = c_D\hat{\rho}\hat{X}^2/\hat{T}^2$, equation (3.4) has the non-dimensional form

$$q_e(u) = \left(u^2 - u_c^2\right)^{m/2}\Theta\left(u^2 - u_c^2\right). \tag{3.5}$$

Typical values of m are $m = 2$ for cohesive sediment and $m = 3$ for non-cohesive sediment, although a very wide range of values have been used (Garcia & Parker 1991).

An alternative erosion model was obtained by Garcia & Parker (1991) using data from open-channel flow experiments with non-cohesive sediment. In this model, the erosion rate $\hat{q}_e$ is written in terms of a dimensionless friction velocity Z_u; using the Chezy drag law, it becomes

$$\hat{q}_e = \hat{w}_s\frac{0.3\beta Z_u^5}{0.3 + \beta Z_u^5}, \qquad \text{where} \quad Z_u = c_D^{1/2}\frac{\bar{u}}{\hat{w}_s}\left(\frac{(\hat{g}_s')^{1/2}\hat{D}_s^{3/2}}{\hat{\nu}}\right)^{3/5}. \tag{3.6}$$

Here $\beta = 1.3\times10^{-7}$ is an empirically fitted constant, $\hat{D}_s$ is the sediment grain diameter, $\hat{\nu}$ is the kinematic viscosity of water and $\hat{g}_s' = \hat{g}(\hat{\rho}_s - \hat{\rho})/\hat{\rho}$ is the reduced gravity of the

sedimentary particles. Defining $\hat{u}_e = 0.3\hat{w}_s$, the dimensionless erosion rate becomes

$$q_e = \frac{u^5}{\alpha + u^5}, \qquad \text{where} \quad \alpha = \frac{0.3}{\beta c_D^{5/2}} \left(\frac{\hat{w}_s \hat{T}}{\hat{X}} \right)^5 \left(\frac{\hat{\nu}}{\hat{D}_s^{3/2} (\hat{g}_s')^{1/2}} \right)^3. \tag{3.7}$$

Using Stokes' law to express $\hat{w}_s$ in terms of $\hat{D}_s$, we may write α as

$$\alpha = \frac{0.3}{18^4 \beta} \frac{1}{c_D^{1/2} (\sin\theta)^2} \frac{\hat{D}_s^{7/2} (\hat{g}_s')^{5/2}}{\hat{A} \hat{g}^2 \hat{\nu}}. \tag{3.8}$$

Taking representative values $\hat{\nu} = 10^{-6}\,\mathrm{m^2\,s^{-1}}$, $c_D = 0.003$ and $\hat{g}_s' = 16\,\mathrm{m\,s^{-2}}$, we obtain $\alpha \approx 4 \times 10^9\,\mathrm{m^{-3/2}} \hat{D}_s^{7/2} \hat{A}^{-1} (\sin\theta)^{-2}$. For sediment of size $\hat{D}_s \lesssim 10^{-3}\,\mathrm{m}$ and for any reasonably large flow event ($A \gtrsim 10^3\,\mathrm{m^3}$) and steep slope ($\sin\theta \gtrsim 0.01$), α will be of order unity or less despite the large dimensional prefactor, but it varies strongly with the size of the sediment and of the surge.

3.1.1. *Some properties of the concentration field*

For the problem described here to be well-posed, it is important that a finite initial concentration can be imposed despite the singularities in u and h as $t \to 0$. We require the asymptotic behaviour of $q_e(u)$ as $u \to \infty$. In this limit, both (3.5) and (3.7) reduce to $q_e \sim u^m$ for some m, and so (3.2) becomes

$$\frac{\mathrm{d}c_\mathrm{L}}{\mathrm{d}t} \sim \frac{u_\mathrm{L}^m}{h_\mathrm{L}} \sim t^{(2-m)/3} \qquad \text{as} \qquad t \to 0. \tag{3.9}$$

Equation (3.9) may be integrated with initial condition $c_\mathrm{L}(0) = 0$ if $(2-m)/3 > -1$, in other words if $m < 5$. This condition is satisfied for all physically realistic erosion models, and so we may regard the problem as well-posed in this respect.

A useful feature of the solution (3.3) is that we can obtain a monotonicity constraint on the concentration field $c(x,t)$. The concentration will increase monotonically towards the front of the flow if $\partial c_\mathrm{L}/\partial k > 0$, and we can write this derivative as

$$\begin{aligned} \frac{\partial c_\mathrm{L}}{\partial k} = \frac{9}{4k^2} \int_0^t \exp\left[\frac{27}{20} \frac{\left(\tau^{5/3} - t^{5/3}\right)}{k^2} \right] \tau^{2/3} \Bigg\{ & -\frac{2}{k} q_e(u_\mathrm{L}(\tau;k)) \\ & + \frac{27}{10} \frac{\left(t^{5/3} - \tau^{5/3}\right)}{k^3} q_e(u_\mathrm{L}(\tau;k)) + \frac{2}{3\tau^{1/3}} \frac{\mathrm{d}q_e}{\mathrm{d}u}(u_\mathrm{L}(\tau;k)) \Bigg\} \mathrm{d}\tau. \end{aligned} \tag{3.10}$$

If the term in curly brackets is positive for all $\tau \in (0,t)$ then $\partial c_\mathrm{L}/\partial k > 0$. This condition will in turn be met if

$$2q_e(u_\mathrm{L}) \leqslant \frac{2k}{3\tau^{1/3}} \frac{\mathrm{d}q_e}{\mathrm{d}u}(u_\mathrm{L}) = u_\mathrm{L} \frac{\mathrm{d}q_e}{\mathrm{d}u}(u_\mathrm{L}) \qquad \text{for} \quad \frac{2k}{3t^{1/3}} < u_\mathrm{L} < \infty. \tag{3.11}$$

The condition (3.11) represents a competition, as k increases towards the front, between the effects of higher velocities (and thus more rapid erosion) and greater depths (and thus slower increase of c). For erosion rates of the form (3.5), enhanced erosion wins when $m \geqslant 2$, and (3.11) is satisfied for all positive k and t. However, (3.11) is not satisfied for erosion rates of the form (3.7), since in this case $q_e \sim 1$ as $u \to \infty$. We will see that this affects how we interpret the conditions for bulking up under the two models.

3.2. *Examples of solutions*

We will now present some results for sediment transport under the two erosion models described above. First (§ 3.2.1) we will discuss the suspended sediment concentration

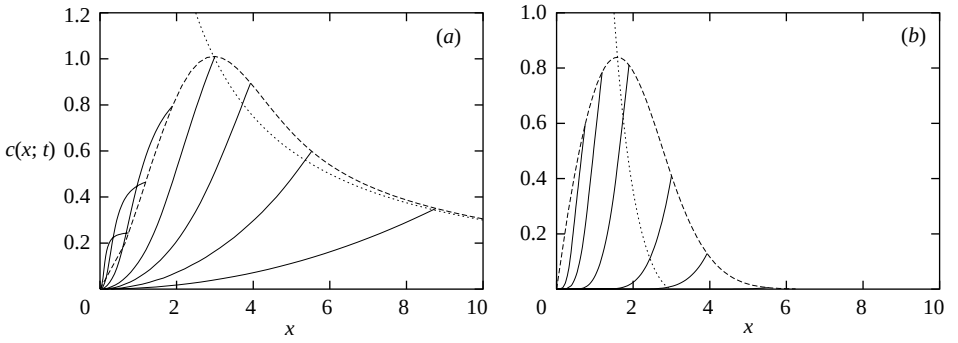

FIGURE 1. Rescaled volumetric concentration $c(x;t)$ under the simple erosion model (3.5) for (*a*) $m=2$ and $u_e=0$; (*b*) $m=3$ and $u_c=1$. Solid lines represent 'snapshots' of concentration field at $t=$ 0.25, 0.5, 1, 2, 5 and 10; dashed lines represent $c_f(t)$; dotted lines represent the equilibrium concentration $c_{\mathrm{eq}}(t)$ at the flow front.

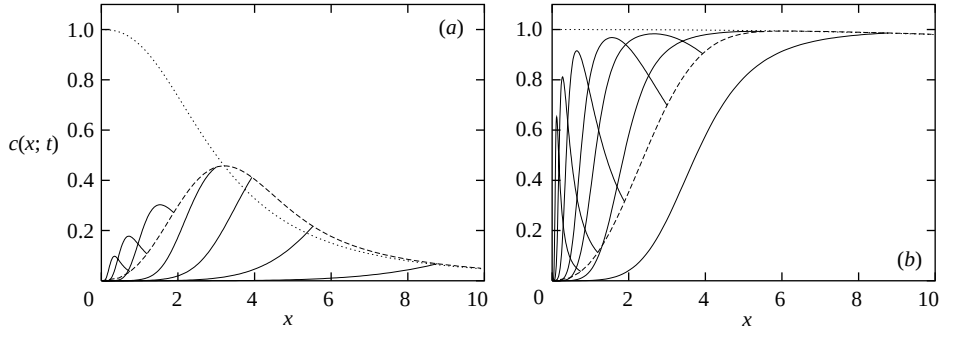

FIGURE 2. Rescaled volumetric concentration $c(x;t)$ under the erosion model (3.7) for (*a*) $\alpha=1$ and (*b*) $\alpha=0.001$. Solid lines represent 'snapshots' of concentration field at $t=$ 0.25, 0.5, 1, 2, 5 and 10; dashed lines represent $c(x_f,t)$; dotted lines represent the equilibrium concentration $c_{\mathrm{eq}}(t)$ at the flow front.

field $c(x,t)$; we will then use this to obtain some simple conditions under which bulking up may be possible (§ 3.2.2); finally we will consider the net scour and deposition under the surge (§ 3.2.3).

3.2.1. *Concentration field* $c(x,t)$

Figure 1 shows typical solutions for $c(x,t)$ and $c_f(t)\equiv c_{\mathrm{L}}(t;k_f)$ under the simple erosion model (3.5), for various values of m and u_c. The most prominent feature is that $c_f(t)$ increases to a maximum value and then gradually decays. This variation in $c_f(t)$ is driven by the rapidly declining 'equilibrium' concentration $c_{\mathrm{eq}}=q_e(u_f)$. At early times the surge is underloaded with sediment (i.e. c is lower than c_{eq}) and so the concentrations increase rapidly. As the surge thins and c_{eq} falls, the frontal concentration overtakes c_{eq}: the flow is now overloaded compared to $c_{\mathrm{eq}}(t)$ and so the concentrations decline. For $m=2$ and $u_c=0$ (figure 1*a*) the decline in c_{eq} is sufficiently gradual for c_f to catch up with c_{eq}, but for $m=3$ and $u_c=1$ (figure 1*b*) the decline of c_{eq} is too fast and the front remains substantially overloaded with sediment for some time.

Figure 2 illustrates the solutions for $c(x,t)$ under the erosion model (3.7). The most obvious difference from figure 1 is that at early stages the concentration is highest

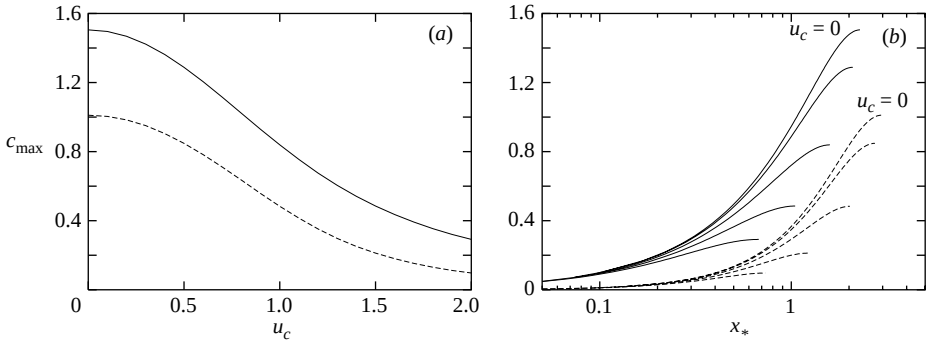

FIGURE 3. (*a*) Maximum concentration $c_{\max}$ attained at the flow front, for $m = 3$ (solid lines) and $m = 2$ (dashed lines) in the simple erosion model (3.5). (*b*) The corresponding positions x_* at which the concentration c_* is first attained, for $m = 3$ (solid lines) and $m = 2$ (dashed lines) with $u_c = 0$, 0.5, 1, 1.5 and 2.

not at the flow front but within the flow. The local maximum gradually catches up with the flow front, and it appears that the maximum concentration attained at the flow front is still the highest ever attained anywhere in the flow. However, if any point in the surge body ever becomes sufficiently turbid for it to behave locally like a laminar muddy flow, this may strongly affect the subsequent behaviour of the flow. It provides, for example, one mechanism by which a single surge may break into successive muddy surges, as is often noticed in the body of a debris flow (Ancey 2001), or by which a relatively clear flow front may outrun a muddy tail, so that the surge divides into two events with quite different properties. While our model is not capable of describing such transitions, this possibility may merit further study.

Considering figure 2, the effect of taking a smaller value of α is that the erosion rate remains close to its maximum value of $q_e = 1$ for longer. Consequently, sediment concentrations increase more rapidly in the early stages of the flow and are sustained for longer in the late stages of the flow, and the maximum concentration attained is closer to its theoretical maximum $c = 1$ ($\hat{c} = 0.3$). As α approaches zero, the erosion rate becomes nearly uniform: $q_e \approx 1$ for almost the entire history of the flow. The limiting case occurs when $\alpha = 0$ and so $q_e = 1$; the solution (3.3) can then be evaluated exactly as

$$c_{\mathrm{L}}(t, k) = 1 - \exp\left(-27t^{5/3}/(20k^2)\right), \tag{3.12}$$

so the maximum concentration $c_{\mathrm{L}} = 1$ is approached over a timescale $t_{\mathrm{m}} \sim k^{6/5}$. (We note that for $\alpha \ll 1$ the model therefore becomes inconsistent very close to the tail of the surge, where $k \ll 1$ and so $\hat{T}k^{6/5} \lesssim \hat{t}_{\mathrm{adj}}$.)

3.2.2. *Maximum concentrations and conditions for the onset of bulking up*

When determining whether the surge will undergo a transition to a muddy flow, the crucial feature of the concentration field is the maximum concentration at a given time. As we have seen, for the simple erosion model (3.5), this maximum is always at the flow front, while for the Garcia–Parker model (3.7), it may occur in the interior of the flow.

We consider first the simple erosion model (3.5). Figure 3(*a*) illustrates how the maximum value of concentration $c_{\max}$ varies with the erosion rate parameters, while figure 3(*b*) shows the minimum distance from source x_* at which a given concentration c_* is first attained. Increasing the erosion threshold u_c reduces $c_{\max}$, as erosion is

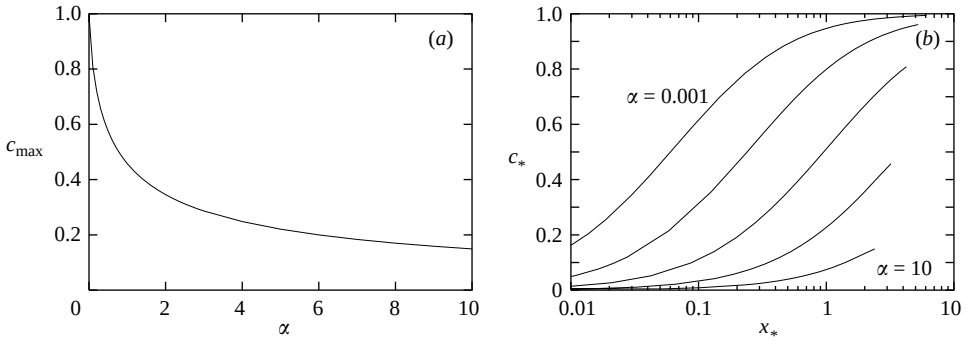

FIGURE 4. (*a*) Maximum concentration $c_{\max}$ attained at any point in the flow at any time using the erosion model (3.7); (*b*) the first point x_* at which the concentration c_* is attained, for $\alpha = 0.001$, 0.01, 0.1, 1 and 10.

progressively restricted to a region close to the flow source. Higher values of m cause the concentration field to peak earlier and at higher values as erosion in the early, high-velocity stage of the flow is enhanced; thus $c_{\max}$ is higher for $m = 3$ than for $m = 2$.

The simplest criterion we can employ for the onset of bulking up is that the maximum concentration reaches some critical value $\bar{c} = \hat{c}_*$ at some point during the surge, where (as noted in § 1) we may take $\hat{c}_*$ to be around 10 %. This criterion provides two necessary conditions for bulking up to occur: first, that the maximum concentration $c_{\max}$ ever attained under the surge is greater than c_*; and second, that the length of the slope on which the surge occurs is sufficient for this concentration to be reached during the lifetime of the surge.

Using figure 3(*a*) or 4(*a*), we can first determine whether $c = c_*$ can be attained at all for a given surge. We can then use figure 3(*b*) or 4(*b*) to determine the minimum distance from source $x_*(c_*; m, u_c)$ at which this concentration is attained; a slope length of at least $x_* \hat{X}$ is then required for the flow to bulk up.

Figure 3(*a*) indicates that for low values of u_c, corresponding to large surges, the maximum concentrations attained under the surge are no greater than around $1.6\hat{C} = 1.6\hat{u}_e/\hat{w}_s$. Consequently, if the ratio $\hat{u}_e/\hat{w}_s$ is less than around 0.06, this erosion model predicts that the surge cannot bulk up through sediment entrainment.

If $\hat{C}$ is large enough for bulking up to occur, it is still necessary for the slope to be long enough for a critical concentration $\hat{c}_*$ to be attained. If c_* is of order 1, then figure 3(*b*) indicates that (at least for low values of u_c) the required dimensionless distance x_* is of order 1. However, if the ratio $\hat{u}_e/\hat{w}_s$ is large, so that turbidity starts to affect the flow for very small values of c_*, then x_* is correspondingly reduced; if c_* is less than about 0.1, then x_* is also less than 0.1 for both values of m, and bulking up may occur on a rather shorter slope than the purely dimensional estimate $\hat{X}$ would suggest.

Figures 4(*a*) and 4(*b*) show the corresponding results for the erosion model (3.7). The major difference is that $x_*(c_*; \alpha)$ is generally less than the distance the flow front has travelled at this point, since c_* may be attained first in the interior of the flow. In general, the pattern of the results is rather similar. For small surges ($\alpha \gtrsim 5$), it is unlikely that the surge can bulk up at all. For $\alpha \gtrsim 0.1$, $\hat{X}$ provides a reasonable estimate of the minimum length of slope required for the flow to bulk up, while for smaller α (large surges) the model suggests that $\hat{X}$ is a considerable overestimate.

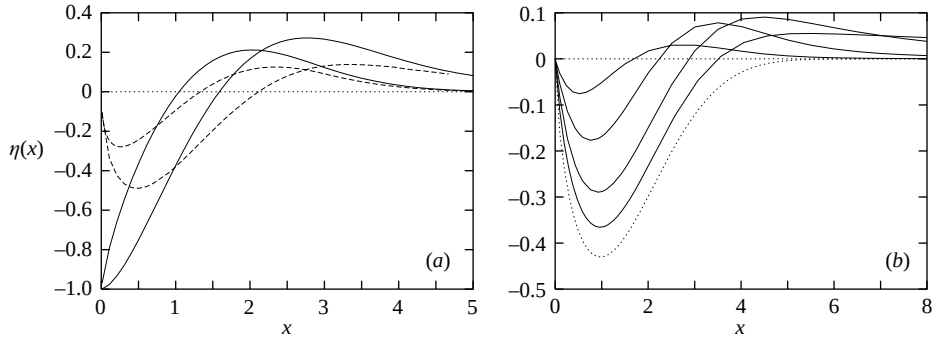

FIGURE 5. Net deposit thickness $\eta(x)$ for (*a*) the erosion model (3.5) with $m = 3$ (solid lines) and $m = 2$ (dashed lines) and with $u_c = 0$ (most scour) and $u_c = 1$; and (*b*) the model (3.7) with $\alpha = 10$ (least scour) to 0.01 (most scour). In (*b*) the dotted line represents the limiting case $\eta_{\alpha=0}(x)$.

3.2.3. *Net scour and deposition*

We now consider the patterns of net scour and deposition predicted by equation (2.12); these will be fully valid only if the surge does not bulk up into a mudflow with rather different erosional properties. Figure 5 shows how the pattern of net scour and deposition alters with the parameters of the erosion models. In each case, net scour occurs close to the source, where velocities are highest, and the eroded material is dumped in a gradually thinning deposit downstream.

Figure 5(*a*) shows the pattern of net scour and deposition under the simple erosion model (3.5). As m and u_c are varied, the shape of the deposit changes, but in all cases the length of the eroded region is between about $\hat{X}$ and $2\hat{X}$. The behaviour as $x \to 0$ is different for $m = 2$ (for which $\eta(x) \to 0$) and $m = 3$ (for which $\eta(x) \to 1$), and the higher value of m gives slightly more erosion overall, but the maximum depth of the scour is bounded in each case by $|\hat{\eta}| = \hat{D}$ (i.e. $|\eta| = 1$).

The results for the Garcia–Parker erosion model (3.7) are shown in figure 5(*b*). As α is decreased, initial scour is increased and deposition is inhibited, so the upstream scour pit becomes deeper and the deposit thins more gradually downstream. Using the result (3.12) for the limiting case $\alpha = 0$, we may obtain

$$\eta_{\alpha=0}(x) = -\frac{20^{1/3}}{9} x^{2/3} \Gamma\left(\frac{1}{3}, \frac{27}{20}\frac{x^{5/2}}{k_f^{9/2}}\right). \tag{3.13}$$

In this limit the model predicts no net deposition downstream: the limiting maximum depth of the scour pit is around $0.43\hat{D}$, and its spatial extent is roughly $4\hat{X}$. The maximum thickness of the downstream deposit for any value of α is about $0.1\hat{D}$.

We note that under both erosion models $|\mathrm{d}\eta/\mathrm{d}x|$ remains an order 1 quantity (except very close to $x = 0$ for $m = 2$), so we are in general justified in neglecting bed level change when calculating the hydrodynamic solution.

4. Concluding remarks

We have used a simple but asymptotically valid model to investigate how rapidly sediment may be entrained into suspension by the flood surge which results when a finite volume of water is released on a slope. Our model only considers the dynamics

of the body of the flow, ignoring the details of the flow front, and is only valid before the suspended sediment load becomes sufficient to affect the flow dynamics. However, this provides us with necessary (though not sufficient) conditions for the flow to bulk up through sediment entrainment. These conditions emerge essentially from the non-dimensionalization of the governing equations: if the characteristic concentration $\hat{C}$ is sufficient to alter the flow dynamics and the length of the slope exceeds the characteristic length $\hat{X}$, the surge may become muddy, and its subsequent history is not predicted by our model. However, using the erosion model of Garcia & Parker (1991) for large, rapid surges, so the parameter α is very small, $\hat{X}$ becomes a considerable overestimate for the length of slope required. In this case the hindmost parts of the surge may become muddy well before the front does, and possibly even during the early stages of flow before the kinematic-wave solution is valid. In contrast to this, a traditional erosion model based on the excess shear stress predicts that the front of the flow will become turbid faster than the tail. This difference in the predictions of the two models suggests the key importance of constraining erosion rates when predicting mudflow initiation, whether using our asymptotic results or any more sophisticated method based on the same physical processes.

We have also presented results for the net erosion and deposition under these surges for the two erosion models considered. In each case, net erosion occurs over a distance of order $\hat{X}$ from the source, while the dimensional quantity $\hat{D}$ provides a reasonable upper estimate for the maximum depth of scour: eroded material is redistributed in a longer and thinner downstream deposit. These results may be of use when assessing the ability of flood surges to reshape natural or artificial channels.

I am grateful to Dr Andrew J. Hogg for bringing the kinematic-wave solution to my attention and for helpful comments on this problem. This work was supported by postdoctoral fellowships from the Newton Trust and from NERC (NE/B50188X/1).

REFERENCES

Ancey, C. 2001 Debris flows and related phenomena. In *Geomorphological Fluid Mechanics* (ed. N. J. Balmforth & A. Provenzale). Springer.

Dyer, K. R. & Soulsby, R. L. 1988 Sand transport on the continental shelf. *Annu. Rev. Fluid Mech.* **20**, 295–324.

Fraccarollo, L. & Capart, H. 2002 Riemann wave description of erosional dam-break flows. *J. Fluid Mech.* **461**, 183–228.

Garcia, M. & Parker, G. 1991 Entrainment of bed sediment into suspension. *J. Hydr. Engng* **117**, 414–435.

Hogg, A. J. & Pritchard, D. 2004 The effects of hydraulic resistance on dam-break and other shallow inertial flows. *J. Fluid Mech.* **501**, 179–212.

Huang, X. & Garcia, M. H. 1998 A Herschel–Bulkley model for mud flow down a slope. *J. Fluid Mech.* **374**, 305–333.

Hunt, B. 1982 Asymptotic solution for dam-break problem. *J. Hydr. Div. ASCE* **108**(HY1), 115–126.

Hunt, B. 1984 Perturbation solution for dam-break floods. *J. Hydr. Engng* **110**, 1058–1071.

Pritchard, D. & Hogg, A. J. 2002 On the transport of fine sediment under dam-break flow. *J. Fluid Mech.* **473**, 265–274.

Teisson, C., Ockenden, M., Le Hir, P., Kranenburg, C. & Hamm, L. 1993 Cohesive sediment transport processes. *Coastal Engng* **21**, 129–162.

Weir, G. J. 1983 The asymptotic behaviour of simple kinematic waves of finite volume. *Proc. R. Soc. Lond.* A **387**, 459–467.